

REPORT DOCUMENTATION PAGE					Form Approved OMB No. 0704-0188	
<p>The public reporting burden for this collection of information is estimated to average 1 hour per response, including the time for reviewing instructions, searching existing data sources, gathering and maintaining the data needed, and completing and reviewing the collection of information. Send comments regarding this burden estimate or any other aspect of this collection of information, including suggestions for reducing the burden, to Department of Defense, Washington Headquarters Services, Directorate for Information Operations and Reports (0704-0188), 1215 Jefferson Davis Highway, Suite 1204, Arlington, VA 22202-4302. Respondents should be aware that notwithstanding any other provision of law, no person shall be subject to any penalty for failing to comply with a collection of information if it does not display a currently valid OMB control number.</p> <p><b>PLEASE DO NOT RETURN YOUR FORM TO THE ABOVE ADDRESS.</b></p>						
1. REPORT DATE (DD-MM-YYYY)		2. REPORT TYPE			3. DATES COVERED (From - To)	
1/16/1996		Conference Paper - Published version			1/1/0001 - 1/1/0001	
4. TITLE AND SUBTITLE PDF CALCULATIONS FOR SWIRL COMBUSTORS				5a. CONTRACT NUMBER		
				5b. GRANT NUMBER		
				5c. PROGRAM ELEMENT NUMBER		
6. AUTHOR(S) harold, james, , Sr lane, lois, , tower, high, ,				5d. PROJECT NUMBER		
				5e. TASK NUMBER		
				5f. WORK UNIT NUMBER		
7. PERFORMING ORGANIZATION NAME(S) AND ADDRESS(ES) RAND CORP SANTA MONICA CA SANTA MONICA CA 90407 242 PRINCETON UNIV NJ PRINCETON NJ 08540 242 HUGHES AIRCRAFT CO CULVER CITY CA CULVER CITY CA 00000 242				8. PERFORMING ORGANIZATION REPORT NUMBER ''		
9. SPONSORING/MONITORING AGENCY NAME(S) AND ADDRESS(ES) HUGHES AIRCRAFT CO CULVER CITY CA CULVER CITY 5 00000				10. SPONSOR/MONITOR'S ACRONYM(S)		
				11. SPONSOR/MONITOR'S REPORT NUMBER(S)		
12. DISTRIBUTION/AVAILABILITY STATEMENT 2 10/9/2015 4:00:00 AM HUGHES AIRCRAFT CO CULVER CITY CA CULVER CITY CA						
13. SUPPLEMENTARY NOTES						
14. ABSTRACT						
15. SUBJECT TERMS						
16. SECURITY CLASSIFICATION OF:			17. LIMITATION OF ABSTRACT	18. NUMBER OF PAGES	19a. NAME OF RESPONSIBLE PERSON	
a. REPORT U	b. ABSTRACT U	c. THIS PAGE			19b. TELEPHONE NUMBER (Include area code)	

# High-performance 1.5 $\mu\text{m}$ GaInNAsSb lasers grown on GaAs

S.R. Bank, M.A. Wistey, L.L. Goddard, H.B. Yuen, H.P. Bae and J.S. Harris

Substantially reduced threshold current density and improved efficiency in long-wavelength ( $>1.4 \mu\text{m}$ ) GaAs-based lasers are reported. A  $20 \times 1220 \mu\text{m}$  as-cleaved device showed a room temperature continuous-wave threshold current density of  $580 \text{ A/cm}^2$ , external efficiency of 53%, and 200 mW peak output power at  $1.5 \mu\text{m}$ . The pulsed threshold current density was  $450 \text{ A/cm}^2$  with 1145 mW peak output power.

**Introduction:** Since the initial demonstration by Fischer and coworkers of a GaInNAs laser at  $1.52 \mu\text{m}$  [1], substantial improvements in device performance have recently been reported [2–6]. Despite this rapid improvement, the threshold current density and external efficiency have remained insufficient for commercial applications. Specifically, only a few continuous-wave (CW) devices have been reported, with threshold current densities remaining above  $1 \text{ kA/cm}^2$  and external efficiencies  $\sim 30\text{--}40\%$ . Owing to the non-reactive nature of  $\text{N}_2$ , an RF plasma cell is typically employed to generate reactive nitrogen for molecular beam epitaxy (MBE) growth. Recent improvements in growth technology have focused on eliminating the ion-related damage generated during active-layer growth [7]. By further reducing the non-radiative recombination rate, we demonstrate substantially improved laser performance at  $1.5 \mu\text{m}$ , at maximum output power. The room temperature pulsed threshold current density of  $450 \text{ A/cm}^2$  for a  $20 \times 1220 \mu\text{m}$  as-cleaved device is equal to the lowest reported GaInNAsSb laser threshold at any emission wavelength [8]. Other room-temperature performance metrics also represent significant improvements over previous reports [6]. The characteristic temperatures for the threshold current density ( $T_0$ ) and external efficiency ( $T_1$ ) were 73 and 125K, respectively. Hole leakage is identified as the primary temperature destabilising mechanism responsible for the reduced  $T_0$  and  $T_1$ . These results are not only encouraging for the prospects for GaAs-based lasers at  $\sim 1.55 \mu\text{m}$ , but are also of significant interest for Raman amplifier applications in the S, C and L bands. Raman amplifiers are more efficient than erbium-doped fibre amplifiers when the pump power exceeds  $\sim 300 \text{ mW}$ .

**Fabrication:** Ridge-waveguide lasers were grown by solid-source MBE on a (100)  $n$ -type GaAs wafer. The growth and fabrication are quite similar to those described in [6]. Group III sources were supplied by effusion cells. Dimeric arsenic was supplied with a conventional valved cracker cell and monomeric antimony with an unvalved cracker cell. An RF plasma cell was used to generate reactive nitrogen. Deflection plates at the exit aperture of the cell, biased at  $-40 \text{ V}$  and ground, were used to minimise the ion flux upon the wafer [7]. Dopants were supplied by silicon ( $n$ -type) and carbon tetrabromide ( $p$ -type).

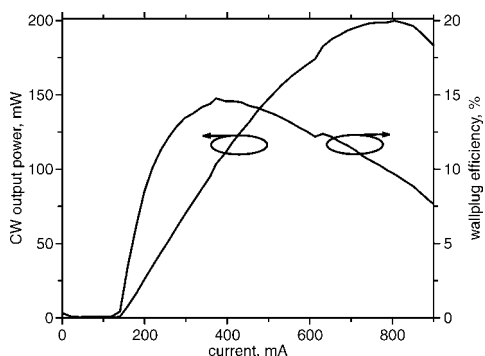


**Fig. 1** Room temperature CW  $L$ - $I$  and wallplug efficiency for  $20 \times 1222 \mu\text{m}$  device

The active layer was a single  $75 \text{ \AA}$   $\text{Ga}_{0.62}\text{In}_{0.38}\text{N}_{0.023}\text{As}_{0.95}\text{Sb}_{0.027}$  quantum well (QW) surrounded on either side by  $220 \text{ \AA}$   $\text{Ga}_{0.975}\text{As}_{0.025}$  barriers grown at  $\sim 440^\circ\text{C}$  and embedded in a  $\text{GaAs}/\text{Al}_{0.33}\text{Ga}_{0.67}\text{As}$  waveguide. The lasers were *ex situ* annealed at  $740^\circ\text{C}$  for 1 min in a rapid thermal annealing furnace, with arsenic out diffusion minimised by a proximity cap. Ridges were defined with lift-off of

Ti/Pt/Au ohmic contacts, followed by a self-aligned dry etch to the top of the GaAs-waveguide. Samples were then thinned to  $\sim 120 \mu\text{m}$  and Au/Ge/Ni/Au was evaporated onto the substrate side. A contact sinter was performed at  $410^\circ\text{C}$  for 1 min. Devices were manually cleaved and mounted epi-side up on a temperature-controlled copper heatsink.

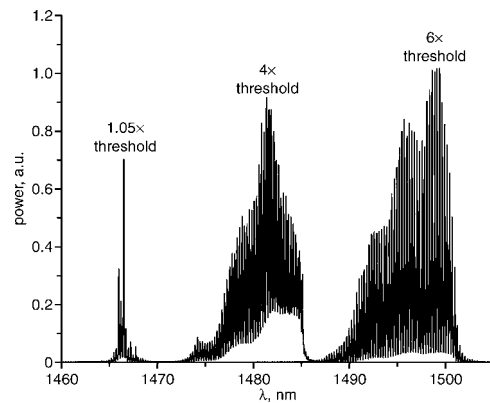


**Fig. 2** Optical spectrum at room temperature for  $20 \times 1222 \mu\text{m}$  device at various levels above threshold

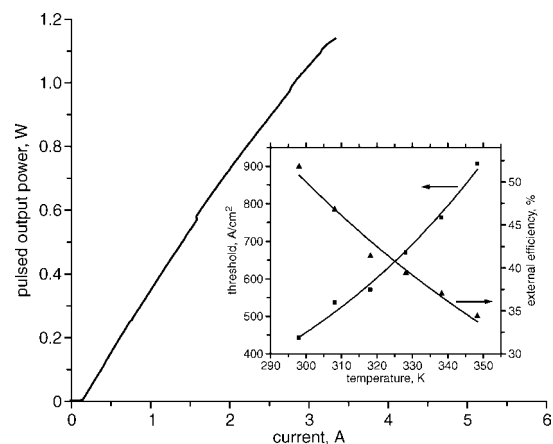


**Fig. 3** Pulsed  $L$ - $I$  curve for  $20 \times 1222 \mu\text{m}$  device at room temperature

Inset: Pulsed threshold current density (squares) and external efficiency (triangles) with temperature

**Results:** Fig. 1 shows the room temperature CW  $L$ - $I$  curve and wallplug efficiency for a  $20 \times 1200 \mu\text{m}$  device with as-cleaved facets. The threshold current density was  $580 \text{ A/cm}^2$ , the external efficiency was 53%, and the peak output power was 200 mW from both facets. A peak CW wallplug efficiency of 14.8% was measured at 103 mW of output power. As shown in Fig. 2, the device lased at  $1.466 \mu\text{m}$  at threshold and redshifted to  $1.502 \mu\text{m}$  at thermal rollover. Using both the bandgap shift with temperature of  $0.58 \text{ nm/K}$  and the thermal resistance of  $24 \text{ K/W}$ , the active region temperature at thermal rollover was estimated to be  $80\text{--}85^\circ\text{C}$ . Devices lased CW up to  $65^\circ\text{C}$ , at a junction temperature of  $90\text{--}95^\circ\text{C}$ .

Under pulsed operation, the laser produced substantially higher output powers. The room temperature pulsed  $L$ - $I$  curve (500 ns pulse, 0.1% duty cycle) is shown in Fig. 3. The threshold current density was  $450 \text{ A/cm}^2$ . The external efficiency was 49% and a driver-limited peak output power of 1.145 W was achieved from both facets. The characteristic temperatures for threshold current density ( $T_0$ ) and external efficiency ( $T_1$ ) were 73 and 125K, respectively, as shown in the inset of Fig. 3. These values are lower than those reported in [6], indicating that carrier leakage may be the dominant non-radiative process in these devices. While the monomolecular recombination rate is substantially reduced, the threshold carrier density is likely to be unchanged. As a result, the rate of carrier leakage is not reduced, resulting in a degradation of both  $T_0$  and  $T_1$ . While further study is required, carrier leakage and not Auger recombination may be the dominant temperature destabilising effect in these devices. No ‘kinks’ were observed in either the threshold current density or external efficiency with temperature. Such behaviour was previously attributed to the turn-on of Auger recombination in similar devices [6]. At  $55^\circ\text{C}$ , the  $Z$ -parameter at threshold,  $Z_{th}$ , was 3.3 [9], confirming the presence of carrier leakage. Auger recombination scales with the cube of the carrier density [10], but carrier

leakage scales with the third or fourth power of the carrier density [11]. Therefore,  $Z_{th} > 3$  must be caused, at least in part, by carrier leakage. Further, photorefectance measurements of identical QW structures show the valence band offset between GaInNAsSb and GaNAs to be  $\sim 50$ – $60$  meV, indicating that holes are the species responsible for the leakage effects.

**Conclusions:** We have demonstrated the first high-performance dilute nitride laser beyond  $1.4\ \mu\text{m}$ . The pulsed threshold current density of  $450\ \text{A}/\text{cm}^2$  is equal to the lowest reported value for a GaInNAsSb laser at any wavelength and  $>2\times$  lower than any previously reported GaAs-based device beyond  $1.4\ \mu\text{m}$ . Under room temperature CW operation the threshold current density was  $580\ \text{A}/\text{cm}^2$ , the external efficiency was 53%, and the peak output power was 200 mW at  $1.5\ \mu\text{m}$ . A significantly higher pulsed output power of 1.145 W was obtained from the same single QW device at room temperature. These performance characteristics all represent a significant improvement over the previous state-of-the-art dilute nitride lasers in the  $1.5\ \mu\text{m}$  regime. Hole leakage was identified as the dominant mechanism governing the temperature sensitivity.

**Acknowledgments:** The authors acknowledge R. Kudrawiec and J. Misiewicz of Wroclaw University of Technology for photorefectance measurements. The authors also thank S. Zou of Santur Corp. for assistance in wafer thinning and A. Moto of Sumitomo Electric Industries for helpful discussions and donation of substrates. This work was supported under DARPA and ARO contracts, DAAD17-02-C-0101, and DAAD199-02-1-0184, and the Stanford Network Research Center (SNRC).

© IEE 2004

19 July 2004

Electronics Letters online no: 20046270

doi: 10.1049/el:20046270

S.R. Bank, M.A. Wistey, L.L. Goddard, H.B. Yuen, H.P. Bae and J.S. Harris, Jr (Solid State and Photonics Lab, Stanford University, Stanford, CA 94305, USA)

E-mail: sbank@stanford.edu

## References

- 1 Fischer, M., Reinhardt, M., and Forchel, A.: 'GaInAsN/GaAs laser diodes operating at  $1.52\ \mu\text{m}$ ', *Electron. Lett.*, 2000, **36**, (14), pp. 1208–1209
- 2 Ha, W., Gambin, V., Bank, S., Wistey, M., Yuen, H., Kim, S.M., and Harris, J.S.: 'Long-wavelength GaInNAs(Sb) lasers on GaAs', *IEEE J. Quantum Electron.*, 2002, **38**, (9), pp. 1260–1267
- 3 Li, L.H., Sallet, V., Patriarche, G., Largeau, L., Bouchoule, S., Merghem, K., Travers, L., and Harmand, J.C.: ' $1.5\ \mu\text{m}$  laser on GaAs with GaInNAsSb quinary quantum well', *Electron. Lett.*, 2003, **39**, (6), pp. 519–520
- 4 Gollub, D., Moses, S., Fischer, M., and Forchel, A.: ' $1.42\ \mu\text{m}$  continuous-wave operation of GaInNAs laser diodes', *Electron. Lett.*, 2003, **39**, (10), pp. 777–778
- 5 Bank, S.R., Wistey, M.A., Yuen, H.B., Goddard, L.L., Ha, W., and Harris, J.S. Jr.: 'Low-threshold CW GaInNAsSb/GaAs laser at  $1.49\ \mu\text{m}$ ', *Electron. Lett.*, 2003, **39**, (20), pp. 1445–1446
- 6 Bank, S.R., Wistey, M.A., Goddard, L.L., Yuen, H.B., Lordi, V., and Harris, J.S. Jr.: 'Low-threshold, continuous-wave,  $1.5\ \mu\text{m}$  GaInNAsSb lasers grown on GaAs', *IEEE J. Quantum Electron.*, 2004, **40**, (6), pp. 656–664
- 7 Wistey, M.A., Bank, S.R., Yuen, H.B., and Harris, J.S. Jr.: 'Real-time measurements of GaInNAs nitrogen plasma ion flux'. Proc. 2003 North American MBE Conf., Keystone, CO, USA, p. 133
- 8 Setiagung, S., Shimizu, H., Ikenaga, Y., Kumada, K., and Kawakawa, A.: 'Very low threshold current density of  $1.3\text{--}\mu\text{m}$ -range GaInNAsSb-GaAs 3 and 5 QWs lasers', *IEEE J. Sel. Top. Quantum Electron.*, 2003, **9**, (5), pp. 1209–1213
- 9 Goddard, L.L., Bank, S.R., Wistey, M.A., Yuen, H.B., Bae, H.P., and Harris, J.S. Jr.: 'Reduced monomolecular recombination in GaInNAsSb/GaAs lasers at  $1.5\ \mu\text{m}$ '. To be presented at IEEE LEOS 2004
- 10 Sweeney, S.J., Phillips, A.F., Adams, A.R., O'Reilly, E.P., and Thijs, P.J.A.: 'The effect of temperature dependent processes on the performance of  $1.5\text{--}\mu\text{m}$  compressively strained InGaAs(P) MQW semiconductor diode lasers', *IEEE Photonics Technol. Lett.*, 1998, **10**, (8), pp. 1076–1078
- 11 Olshansky, R., Su, C.B., Manning, J., and Powazinik, W.: 'Measurement of radiative and nonradiative recombination rates in InGaAsP and AlGaAs light sources', *IEEE J. Quantum Electron.*, 1984, **QE-20**, (8), pp. 838–854